

Kinetics of the field-induced resistivity jump in $\text{Ni}_2\text{Mn}_{1.36}\text{Sn}_{0.64-x}\text{Ga}_x$ alloys

S. Chatterjee,¹ S. Giri,¹ S. K. De,² and S. Majumdar^{1,*}

¹*Department of Solid State Physics, Indian Association for the Cultivation of Science,
2A & B Raja S. C. Mullick Road, Jadavpur, Kolkata 700 032, India*

²*Department of Materials Science, Indian Association for the Cultivation of Science,
2A & B Raja S. C. Mullick Road, Jadavpur, Kolkata 700 032, India*

(Received 11 September 2009; revised manuscript received 25 May 2010; published 25 June 2010)

We report here the observation of field-induced jump in resistivity in Ga-doped Ni-Mn-Sn shape memory alloy ($\text{Ni}_2\text{Mn}_{1.36}\text{Sn}_{0.64-x}\text{Ga}_x$, $x=0.32$ and 0.36). The samples order ferromagnetically at around 330 K and undergo martensitic transition near room temperature or below. The observed jump shows interesting kinetic behavior with the manifestation of strong relaxation as a function of time. A model based on the multiple free-energy minima between the parent and product phases has been mooted to account for the time variation in the jump which is otherwise supposed to be athermal in character.

DOI: [10.1103/PhysRevB.81.214441](https://doi.org/10.1103/PhysRevB.81.214441)

PACS number(s): 81.30.Kf, 64.60.My, 61.20.Lc

I. INTRODUCTION

Martensitic transition (MT) is generally athermal in nature, i.e., it only takes place when the system is driven by external parameters such as temperature (T), magnetic field (H), or pressure (P).^{1,2} Being nondiffusive, large strain energy is involved in the transition and consequently, the system has to overcome a huge free energy barrier separating the minima corresponding to the parent phase and the more stable product phase. The transition takes place for certain values of the external parameters and it is generally time independent, i.e., amount of transformed phase does not depend upon incubation time (no relaxation) or the rate of change in the external parameters. In a real material, the free-energy landscape is quite complex due to the presence of disorder^{3–5} and there exist multiple metastable states. While the system is evolving through these metastable states, the transformation can occur through single or multiple jumps or avalanches in order parameter, which takes place in a very short (or no) time scale.⁶

There are few instances where aging can affect the transition, and they are referred as isothermal MT. The well-known examples are Cu-Al-Ni, Fe-Ni-Mn, Fe-Ni, Ti-Ni alloys,^{2,7,8} and some doped manganites.⁹ Kakeshita *et al.*^{7,8} have proposed and successfully applied a probabilistic model for the isothermal MT, which is based on the thermal fluctuation assisted process to overcome the free-energy barrier. In the present paper, we report the occurrence of field-induced first-order jump in resistivity in some Heusler-type Ni-Mn-Sn-Ga alloys with unusual time dependence. So far Ni-Mn-Ga alloys are the most studied materials among the ferromagnetic shape memory alloys.¹⁰ On the other hand, Ni-Mn-Sn alloys have recently attracted considerable attention,¹¹ where magnetic field induced transition near the T -driven MT plays the pivotal role for their magnetofunctional properties.¹² Here we shall focus on the solid solution of Ni-Mn-Sn and Ni-Mn-Ga alloys ($\text{Ni}_2\text{Mn}_{1.36}\text{Sn}_{0.64-x}\text{Ga}_x$, $x=0$, 0.32 , and 0.36), which can be thought of being derived from $\text{Ni}_2\text{Mn}_{1.36}\text{Sn}_{0.64}$ (Refs. 13 and 14) by the replacement of Sn with Ga. Our main aim is to blend the field-induced transition of Ni-Mn-Sn alloy with the conventional ferromag-

netic shape memory effect of the Ni-Mn-Ga counterpart. Gradual Ga doping at the Sn site pushes the martensitic transition temperature (T_M) to higher values and for $x=0.36$, it reaches just above the room temperature. However, the ferromagnetic Curie point (T_C) remains almost constant (close to 330 K).¹⁵ This provides a useful opportunity to study the magnetostructural transition at the elevated temperature, where strong thermal effect is present. In addition, we would like to address change in the nature of the field-induced transition with Ga doping.

II. EXPERIMENTAL DETAILS

The polycrystalline samples of Ni-Mn-Sn-Ga alloys were prepared by argon arc-melting the constituent elements. The samples were subsequently annealed in a sealed quartz tube in vacuum at 900 °C for 43 h followed by rapid quenching in ice water. The room-temperature powder x-ray diffraction (XRD) patterns recorded with Cu $K\alpha$ radiation [see Figs. 1(a) and 1(b)] indicate that for $x=0$ and 0.32 samples, the crystal structure is ordered $L2_1$ type. Even for large Ga doping the ordered $L2_1$ structure prevails in the $x=0.32$ alloy as clear from the existence of (111) and (311) reflections.¹⁶ On the other hand, for the $x=0.36$ sample, two structural phases, namely, cubic austenite ($a=5.91$ Å) and orthorhombic martensite ($a=8.48$ Å, $b=5.55$ Å, and $c=4.35$ Å), coexist together at room temperature. This phase coexistence is due to the occurrence of first-order MT between 270 to 315 K. It is to be noted that the high- T austenite for the Mn excess Heusler compositions $\text{Ni}_2\text{Mn}_{1+\delta}\text{Z}_\delta$ ($\text{Z}=\text{Sn}, \text{Ga}$) is always cubic while the low- T martensite is orthorhombic for the Sn-based alloys. The $x=0.36$ alloy therefore retains the cubic austenite and the orthorhombic martensite structures just like the full Sn composition ($\text{Ni}_2\text{Mn}_{1.36}\text{Sn}_{0.64}$). The cubic lattice parameter (a_c) of the Ga-doped samples varies linearly with x obeying the Vegard's law for alloys formation [see inset of Fig. 1(a), where we have also added a_c of $x=0.24$ and 0.28 , the compositions which are not otherwise discussed in the paper]. None of the sample shows any peak corresponding to unreacted Ga (the prominent Ga peak is supposed to occur at $2\theta=34.94^\circ$).

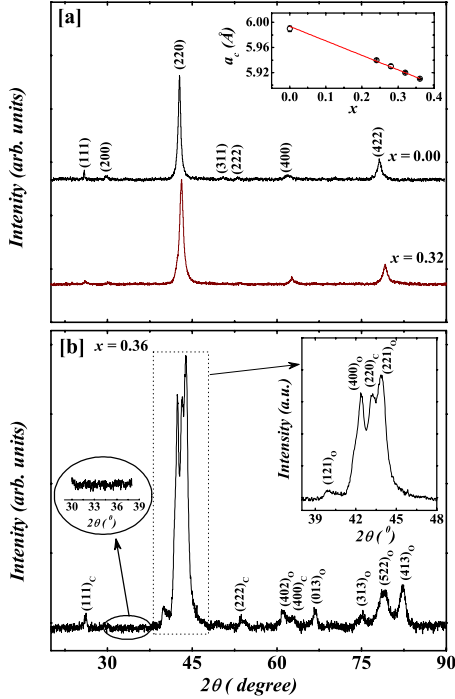


FIG. 1. (Color online) Powder x-ray diffraction pattern of $\text{Ni}_2\text{Mn}_{1.36}\text{Sn}_{0.64-x}\text{Ga}_x$ ($x=0, 0.32, 0.36$) samples recorded at room temperature using $\text{Cu } K\alpha$ radiation. $x=0$ and 0.32 samples show pure cubic $L2_1$ structure while $x=0.36$ sample shows the mixture of $L2_1$ and orthorhombic structures. The subscripts c and o, respectively, denote the indices corresponding to cubic and orthorhombic reflections. The inset of (a) shows the variation in cubic lattice parameter with x .

We performed scanning electron microscopy (SEM) and energy-dispersive x-ray spectroscopy (EDS) at different parts of the samples using JEOL JSM 6700F FESEM. The SEM micrographs for $x=0.36$ sample has been depicted in Fig. 2. Distinct twined variants are visible all over the sample piece, indicating a predominantly martensitic phase at room temperature. This is consistent with the observed orthorhombic phase in the XRD pattern [see Fig. 1(b)]. No signature of unreacted precipitation of the constituent elements and/or secondary phase were observed. The EDS shows homogeneous concentration of the constituent elements within the accuracy of the method. We performed EDS at 15 different regions of the sample ($x=0.36$) with effective scanning area of $0.5 \times 0.5 \text{ mm}^2$. The average Ga stoichiometry was found to be 0.359 with standard deviation 0.015, which is close to the expected value. The XRD, SEM, and EDS observations together rule out the possibility of any Ga precipitation in the sample.

The resistivity (ρ) of the present samples was measured by four-point technique in presence of magnetic field as high as 90 kOe. Both homemade setup fitted in a nitrogen cryostat and a cryogen-free high magnetic field system (Cryogenic Ltd., U.K.) were used for ρ measurements.

III. RESULT AND DISCUSSION

The T variation in ρ for three different compositions has been shown in Fig. 3. Clear thermal hysteresis is observed in

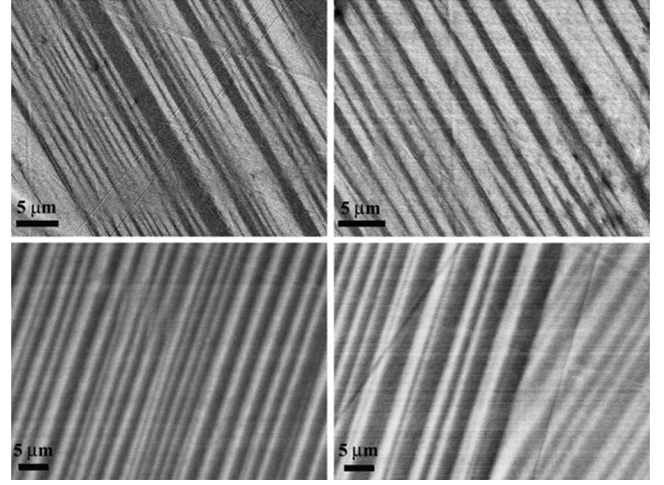


FIG. 2. Representative scanning electron micrographs of $\text{Ni}_2\text{Mn}_{1.36}\text{Sn}_{0.28}\text{Ga}_{0.36}$ recorded at four different regions of the sample piece at room temperature. Twined variants are clearly visible in both the micrographs indicating the sample to be in the martensitic phase.

$\rho(T)$, which signifies the MT between high- T austenite and low- T martensite. The onset of ferromagnetism in the form of a slope change is observed close to $T_C \approx 330 \text{ K}$ for all the samples. Notably, $x=0.32$ and 0.36 samples show large training effect when thermally cycled through the MT. In the inset of Figs. 3(b) and 3(c), we have plotted $\rho(T)$ for the first, fifth, and tenth cycles. The cooling line crosses the heating data just below the MT and it remains above the heating line down to the lowest T of measurement. The absolute magnitude of ρ increases gradually both in the austenite and the martensite with thermal cycling. However, ρ approaches to an equilibrium value for sufficient number of cycling (roughly 20). No such cycling effect is present in the pure Sn sample ($x=0.0$). In the main panel of Figs. 3(b) and 3(c), we have plotted $\rho(T)$ for the 25 times cycled sample, and the training effect is negligible here. The ρ versus H data presented in the subsequent part of the paper were measured both on *trained* samples (thermally cycled 25 times) as well as on uncycled *pristine* samples for the $x=0.32$ and $x=0.36$ compositions.

In our previous work on $\text{Ni}_2\text{Mn}_{1.36}\text{Sn}_{0.64}$ sample with MT occurring around 110 K, the applied H causes ρ to decrease smoothly resulting large magnetoresistance $\{\text{MR}=[\rho(H)-\rho(0)]/\rho(0)\}$.¹⁴ The variation in ρ with H is monotonous without showing much features. The MR in this full Sn sample is found to be highly irreversible with respect to the cycling of H and the sample retains the low resistive state even when H is brought back to zero. Now let us look at the $\rho(H)$ (normalized by the $H=0$ value) behavior of the Ga-doped samples. A comparison has been made between the $\rho(H)$ data of $x=0, 0.32$, and 0.36 samples all measured at temperature T_0 , which is the mean temperature of the end points of the $\rho(T)$ hysteresis loop. Clearly, $\rho(H)$ is markedly different in case of the Ga-doped samples as compared to the undoped alloy [see Fig. 4(a)]. Notably, the Ga-doped alloys show sharp jumplike change in ρ at certain fields while $\rho(H)$ shows a monotonous decrease with H in case of $x=0$ sample.

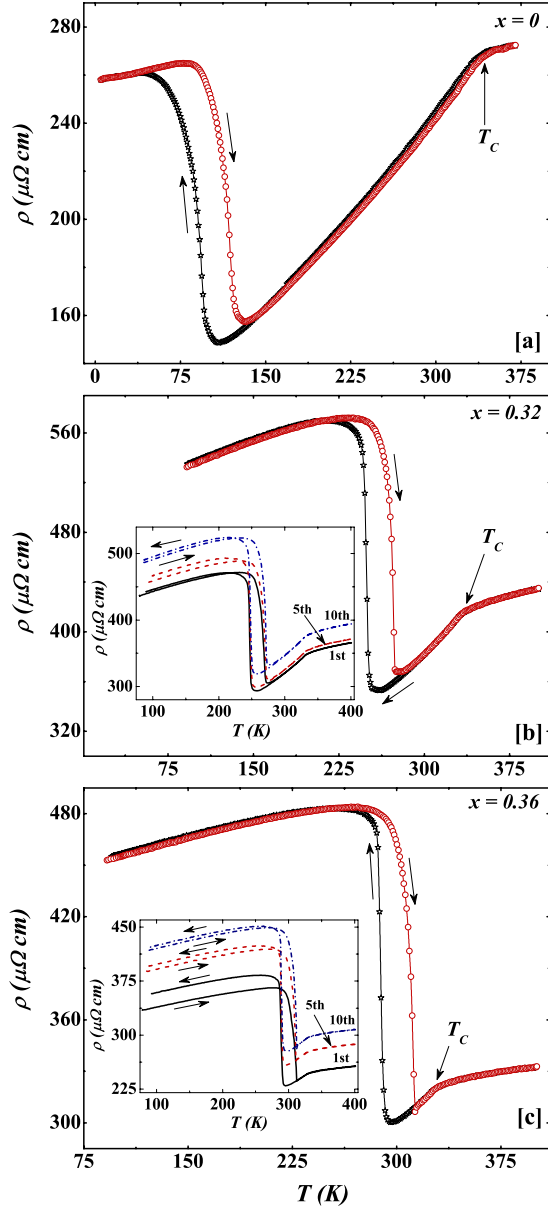


FIG. 3. (Color online) Resistivity is plotted as a function of temperature for both heating and cooling legs (indicated by arrows) for (a) $x=0$, (b) 0.32, and (c) 0.36 samples. The insets of (b) and (c) show the resistivity data for different thermal cycles indicating the training effect.

After the jump occurs, ρ gets arrested in a low resistive state and it remains there for further field cycling. Similar sharp jumps in ρ and M were observed in case of materials showing first-order field-induced transition.^{17–21} The avalanche-like jump near a magnetotransport transition is generally attributed to the competition between magnetic energy and the strain energy associated with the first-order transition.¹⁷ Figure 4(b) shows the normalized ρ versus H data recorded at 308 K on the trained as well as on the pristine samples of $x=0.36$ composition. The field-induced jump is present in both trained and pristine samples, however, observed jump is sharper in case of pristine sample, although it occurs at a higher H . The pristine sample shows small steplike anomaly

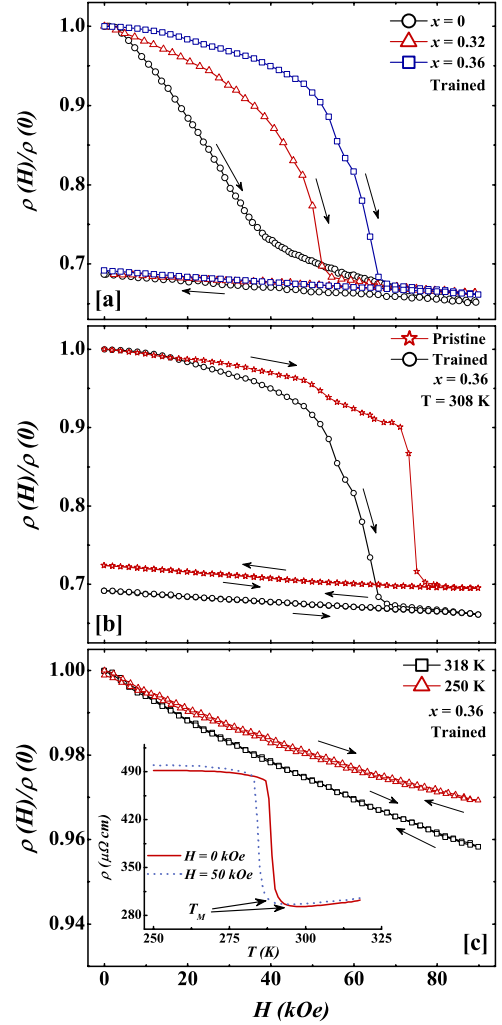


FIG. 4. (Color online) (a) shows the normalized resistivity as a function of field for $x=0$, 0.32, and 0.36 samples measured at the midpoint of their martensitic transition temperatures (T_0). (b) Highlights the field-induced jump in $x=0.36$ alloy for the pristine and the trained samples at 308 K while (c) shows the absence of jump when measured outside the region of martensitic transition. The inset of (c) shows the resistivity versus temperature data of $x=0.36$ for two different applied fields during cooling.

at a lower H , which matches well with the onset of jump in the trained sample. The field-induced jump and the subsequent arrested state is only present within the region of MT. No such effect is observed in the $\rho(H)$ measurement just outside the region of MT as evident from the isotherms recorded at 250 and 320 K [Fig. 4(c)].

The field-induced jump is found to be a unique feature of the Ga-doped compositions, which is not present in the pure Sn sample. However, apart from the jump, doped samples show magnetic and magnetotransport behaviors very similar to that of undoped sample. The notable point of similarities are: (i) $\rho(H)$ shows large irreversibility (open hysteresis loop) between increasing and decreasing field legs. (ii) T_M shifts to lower T under H . The inset of Fig. 4(c) shows the shift of T_M by about 6 K under $H=50$ kOe. (iii) All the Ga-doped samples show positive magnetocaloric effect (not shown here) similar to the Ni-Mn-Z ($Z=\text{In, Sn, Sb}$) alloys.¹⁵

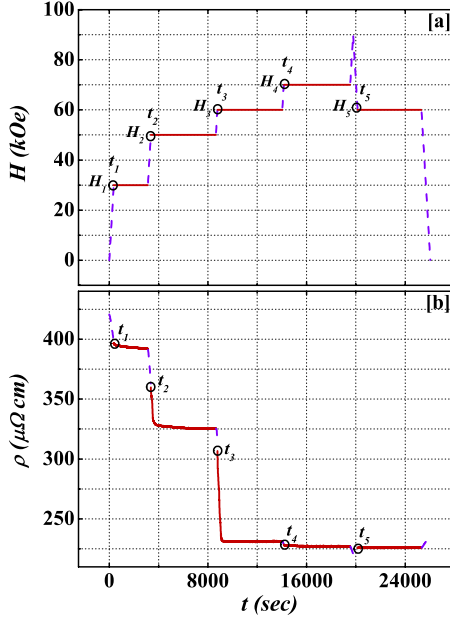


FIG. 5. (Color online) (a) shows the protocol for resistivity measurement in a field-time diagram. t_i ($i=1,2,\dots$) denotes the absolute time where a new constant field H_i is attained. The dashed line shows the field ramping segment while the solid lines are the constant field segment. (b) shows the corresponding change in resistivity as a function of time.

It is well established that Ni-Mn-Z alloys show reverse MT (from martensite to austenite) under H . The observed similarities indicate that the likely scenario for the field-induced transition in $\text{Ni}_2\text{Mn}_{1.36}\text{Sn}_{0.64-x}\text{Ga}_x$ is also a reverse MT.

In order to address the kinetics of the field-induced jump, we investigated the time evolution of ρ at different constant H for the $x=0.36$ sample. The measurement was performed in the following protocol: (i) the sample was first heated to 308 K from a zero-field-cooled state at 200 K, (ii) then H is increased from zero to 90 kOe in a discontinuous manner with intermediate stops at $H_i=30, 50, 60$, and 70 kOe and at each stop we measured the time evolution of ρ , (iii) the field was then ramped down to 60 kOe and relaxation was measured, eventually (iv) the field was ramped down to zero. The protocol is described in Fig. 5(a), where t denotes the absolute time of measurement with $t=0$ being the starting point of section (ii) of the protocol. Here t_i denotes the starting time for the i th relaxation measurement corresponding to the constant field H_i . T was kept constant at 308 K for the whole measurement (maximum fluctuation in T was less than 5 mK). The corresponding variation in ρ has been shown in Fig. 5(b). The magnetic field mentioned in the relaxation data is the *sample site magnetic field* measured *in situ* by a Hall sensor and the maximum fluctuations of the recorded H is found to be within ± 4 Oe.

In Fig. 6(a), we have shown ρ versus t data in a relative scale of time, namely, $(t-t_i)$. For $H_i=30$ kOe, ρ hardly changes with t , with a maximum -0.9% change in 2880 s. When H was increased to 50 kOe, a sharp decrease in ρ was observed. The interesting point is that ρ continued to drop over a finite period of time of about 200 s even after the field got stabilized at 50 kOe, and the observed change in ρ in

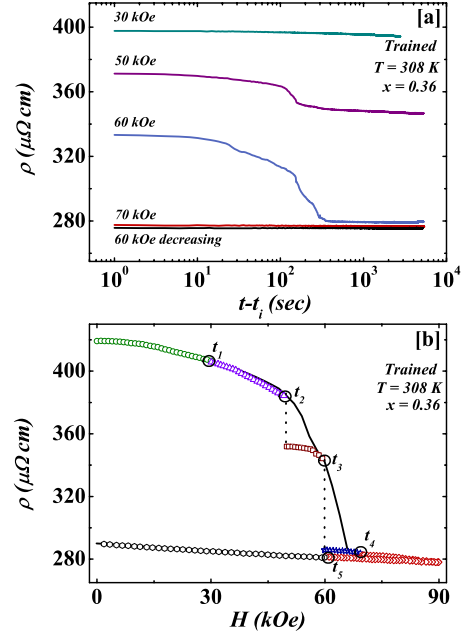


FIG. 6. (Color online) (a) The resistivity of the sample as a function of time at 308 K for different constant applied fields as measured by the protocol described in Fig. 5. (b) shows the resistivity as a function of applied field for uninterrupted data (solid line) and measurement with intermediate stops (data points). The vertical dotted line shows the change in resistivity with waiting time in constant fields.

constant H and T was found to be as high as -6.5% . When the field was increased to 60 kOe, ρ decreased further. Here also ρ relaxed over a finite time window of 300 s beyond stable field of 60 kOe. The relaxation in ρ in constant H and T is much higher at $H_i=60$ kOe (-16% in 300 s). For $H_i=70$ and 60 kOe (on the H decreasing path), no such drop in ρ was observed, indicating the completion of the transition after the application of 60 kOe of field and subsequent waiting. The observed change in ρ for $H_i=50$ and 60 kOe [Fig. 6(a)] indicates that the H -induced MT in the present sample is not purely athermal. $H_i=30$ kOe is too low to induce any transition, whereas at 50 kOe of field, the system became unstable. A partial transition occurred at 50 kOe, whereas the rest of the transition took place at 60 kOe. The strong waiting time dependence of ρ at constant fields of 50 and 60 kOe manifests the role of thermal fluctuation toward the observed effect.

In Fig. 6(b), we have plotted the uninterrupted $\rho(H)$ loop (0–90 kOe and back, solid line) along with the measurements performed with intermediate stops [as described by the protocol in Fig. 5(a)]. Notably, ρ with intermediate stops always tends to follow the uninterrupted line after the relaxation at different points and subsequent field increase. The vertical dotted lines denote the change in ρ with t in constant H . It indicates that the same transition under a ramping field can be achieved by waiting at some constant fields.

It is pertinent to investigate whether the observed jump and the associated temporal effect is common to all first-order field-induced transition in Ni-Mn-based alloys. In order to address this, we measured the time evolution of ρ for

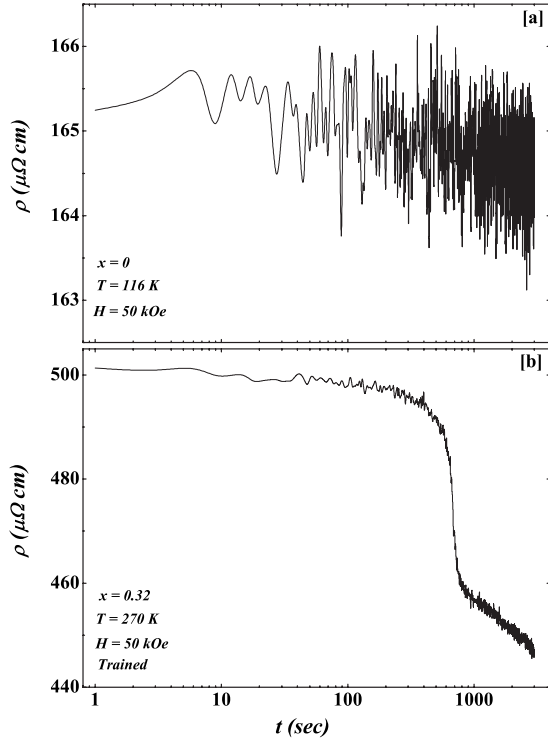


FIG. 7. (a) and (b) show the time-dependent resistivity of $x=0$ and 0.32 samples, respectively, measured at the midpoint of the respective martensitic transitions after the application of 50 kOe of external field.

$x=0$ and 0.32 samples as well. The relaxation measurements were performed at 50 kOe of applied field at the respective T_0 's of the samples. The pure sample does not show any noticeable change in ρ with t and the observed change is within the noise level of measurements [as evident from the fluctuations in Fig. 7(a)]. While the $x=0.32$ sample shows clear jump as a function of t , which occurs 500 s after the application of field [Fig. 7(b)].

The time evolution of ρ is also observed in pure Sn sample in certain protocol of measurements (on field withdrawal after field cooling). However, it is characteristically different from what we observe in case of Ga-doped samples. The pure Sn sample, namely, $\text{Ni}_2\text{Mn}_{1.36}\text{Sn}_{0.64}$ gets arrested in a glassy magnetic state on field cooling (kinetic arrest),¹³ and on field removal, it emerges out of that arrested phase. Such kinetically arrested state is not present in the Ga-doped samples, and the time evolution is solely connected to the slow dynamics of the field-induced transition, not to an arrested glassy phase at low temperature.

The observed field-induced jump is restricted within the region around the thermally driven MT, where the system remains far from equilibrium. On heating the system from pure martensite to T_0 , the system assumes some metastable states within the region of transition. The application of H tends to drive the system from the metastable martensite (\mathcal{M}) to the stable austenite (\mathcal{A}).¹² The direct transition to a more stable configuration by overcoming large energy barrier can be difficult, and the system is likely to proceed through easily accessible local minima.⁵ A possible free-energy scenario with multiple minima has been depicted in Fig. 8,

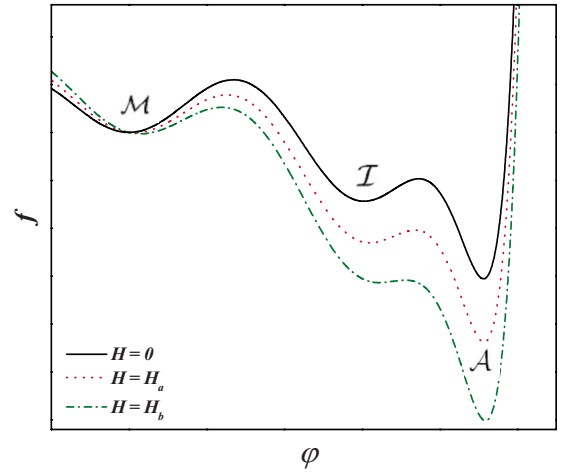


FIG. 8. (Color online) A model for free energy as a function of order parameter (ϕ) for the observed magnetostructural transition at different applied fields ($0 < H_a < H_b$). Here \mathcal{A} and \mathcal{M} denote the minima corresponding to austenite and martensite phases, whereas \mathcal{I} is due to an intermediate phase. Here H_b is a field where the free-energy barrier between \mathcal{I} and \mathcal{A} is quite small compared to the thermal energy ($k_B T$), and the transition can take place instantaneously. On the other hand at H_a , it is comparable to $k_B T$, and the transition is thermally driven with associated relaxation. For $x=0.36$ sample, the probable field ranges (in kilo-oersted) are $30 < H_a \leq 50$ and $60 < H_b \leq 70$.

where for simplicity only one intermediate minimum (\mathcal{I}) between \mathcal{A} and \mathcal{M} is shown. At zero or low field, the free-energy barrier between the states \mathcal{A} and \mathcal{M} is so high that the thermal energy cannot invoke the transition alone. However, an applied magnetic field can reduce the height of the free-energy barrier paving the path for the transition.²² A situation can arise when H is not high enough to induce the full transition. In that case the transition can be two step process, where the system first evolves into an intermediate state (here \mathcal{I}) by the applied field, and then the thermal energy helps the system to reach the final phase \mathcal{A} . This might be the case for the isothermal waiting at 50 or 60 kOe, where H causes a partial transition (from \mathcal{M} to \mathcal{I}) and then the observed relaxation beyond the point of field stabilization is due to the transition across the free-energy barrier between \mathcal{I} and \mathcal{A} assisted by the thermal fluctuations.

We observe several small jumps in ρ when measured as a function of time [Fig. 6(a)] as well as field [Fig. 4(b)]. Such small jumps have been previously observed in other materials near first-order transition (see, for example, Ref. 18). This is believed to occur due to the presence of multiple free-energy minima in the system. Although, in this model (see Fig. 8), we assumed a single intermediate state for simplicity, in practice, the more likely scenario is the multiple intermediate states. This also explains why the jump is less sharper in case of the trained sample. Cycling through the MT creates stress-induced disorder (in the form of microcracks),²³ which enhances the number of intermediate states. As a result, system evolves through more number of intermediate states and the overall transition becomes less sharper.

IV. CONCLUSION

Summarizing, the field-induced jump in resistivity is observed in the Ga-doped Ni-Mn-Sn sample with nominal composition $\text{Ni}_2\text{Mn}_{1.36}\text{Sn}_{0.64-x}\text{Ga}_x$ ($x=0.32, 0.36$). Our study indicates that the observed jump in ρ is not purely athermal (instantaneous) in nature, rather it occurs within a finite window of time. The possible scenario for the above behavior lies in the existence of intermediate free-energy minima,

through which the system proceeds when the field is ramped. Similar time-dependent jump has been observed in few other materials^{9,24} and the same model of intermediate states can also be applied to account for the temporal effect.

ACKNOWLEDGMENT

The present work is financially supported by the CSIR, India.

*sspsm2@iacs.res.in

- ¹A. Planes, F.-J. Pérez-Reche, E. Vives, and L. Mañosa, *Scr. Mater.* **50**, 181 (2004).
- ²K. Otsuka, X. Ren, and T. Takeda, *Scr. Mater.* **45**, 145 (2001).
- ³Y. Imry and M. Wortis, *Phys. Rev. B* **19**, 3580 (1979).
- ⁴J. P. Sethna, K. Dahmen, S. Kartha, J. A. Krumhansl, B. W. Roberts, and J. D. Shore, *Phys. Rev. Lett.* **70**, 3347 (1993).
- ⁵K. Dahmen and J. P. Sethna, *Phys. Rev. B* **53**, 14872 (1996).
- ⁶E. Vives, J. Ortín, L. Mañosa, I. Ràfols, R. Pérez-Magrané, and A. Planes, *Phys. Rev. Lett.* **72**, 1694 (1994).
- ⁷T. Kakeshita, T. Saburi, and K. Shimizu, *Philos. Mag. B* **80**, 171 (2000).
- ⁸T. Kakeshita, J. Katsuyama, T. Fukuda, and T. Saburi, *Mater. Sci. Eng., A* **312**, 219 (2001).
- ⁹V. Hardy, A. Maignan, S. Hébert, C. Yaicle, C. Martin, M. Hervieu, M. R. Lees, G. Rowlands, D. Mc K. Paul, and B. Raveau, *Phys. Rev. B* **68**, 220402(R) (2003).
- ¹⁰J. Enkovaara, A. Ayuela, A. T. Zayak, P. Entel, L. Nordström, M. Dube, J. Jalkanen, J. Impola, and R. M. Nieminen, *Mater. Sci. Eng., A* **378**, 52 (2004).
- ¹¹T. Krenke, M. Acet, E. F. Wassermann, X. Moya, L. Mañosa, and A. Planes, *Nature Mater.* **4**, 450 (2005).
- ¹²K. Koyama, K. Watanabe, T. Kanomata, R. Kainuma, K. Oikawa, and K. Ishida, *Appl. Phys. Lett.* **88**, 132505 (2006).
- ¹³S. Chatterjee, S. Giri, S. Majumdar, and S. K. De, *Phys. Rev. B* **77**, 224440 (2008).
- ¹⁴S. Chatterjee, S. Giri, S. Majumdar, and S. K. De, *J. Phys. D* **42**, 065001 (2009).
- ¹⁵S. Chatterjee, S. Giri, S. Majumdar, and S. De, [arXiv:1003.6116](https://arxiv.org/abs/1003.6116), J. Alloys Compd. (to be published).
- ¹⁶M. Wittmann, I. Baker, and P. R. Munroe, *Philos. Mag.* **84**, 3169 (2004).
- ¹⁷V. Hardy, S. Majumdar, S. Crowe, M. R. Lees, D. McK. Paul, L. Hervé, A. Maignan, S. Hébert, C. Martin, C. Yaicle, M. Hervieu, and B. Raveau, *Phys. Rev. B* **69**, 020407(R) (2004).
- ¹⁸V. Hardy, S. Majumdar, M. R. Lees, D. McK. Paul, C. Yaicle, and M. Hervieu, *Phys. Rev. B* **70**, 104423 (2004).
- ¹⁹F. M. Woodward, J. W. Lynn, M. B. Stone, R. Mahendiran, P. Schiffer, J. F. Mitchell, D. N. Argyriou, and L. C. Chapon, *Phys. Rev. B* **70**, 174433 (2004).
- ²⁰J. Kushauer, R. van Benthum, W. Kleemann, and D. Bertrand, *Phys. Rev. B* **53**, 11647 (1996).
- ²¹A. Haldar, K. G. Suresh, and A. K. Nigam, *Phys. Rev. B* **78**, 144429 (2008).
- ²²A. Asamitsu, Y. Moritomo, R. Kumai, Y. Tomioka, and Y. Tokura, *Phys. Rev. B* **54**, 1716 (1996).
- ²³J. B. Sousa, A. M. Pereira, F. C. Correia, J. M. Teixeira, J. P. Araújo, R. P. Pinto, M. E. Braga, L. Morellon, P. A. Algarabel, C. Magen, and M. R. Ibarra, *J. Phys.: Condens. Matter* **17**, 2461 (2005).
- ²⁴M. K. Chattopadhyay, M. A. Manekar, A. O. Pecharsky, V. K. Pecharsky, K. A. Gschneidner, Jr., J. Moore, G. K. Perkins, Y. V. Bugoslavsky, S. B. Roy, P. Chaddah, and L. F. Cohen, *Phys. Rev. B* **70**, 214421 (2004).